PHYSICAL REVIEW B

CONDENSED MATTER

THIRD SERIES, VOLUME 41, NUMBER 13 PART A 1 MAY 1990

Four-wave mixing of Nd^{3+}-doped crystals and glasses

Richard C. Powell,* Stephen A. Payne, L. L. Chase, and G. D. Wilke

University of California, Lawrence Livermore National Laboratory, P.O. Box 5508, Livermore, California 94550

(Received 6 November 1989)

Degenerate four-wave-mixing measurements have been performed on a wide variety of Nd^{3+}-doped oxide and fluoride glasses and crystals. Crossed beams from a cw argon-ion laser were used to excite the Nd^{3+} ions directly and establish population gratings. Absolute measurements of the signal strengths were made, and their magnitudes were found to be sensitively influenced by the composition of the host. A theoretical model was developed to interpret the results, and it was found that the dominant contribution to the signal is associated with the difference in polarizability of the Nd^{3+} ions in the metastable state versus the ground state. The magnitude of the observed change in the polarizability indicates that the $4f \rightarrow 5d$ transitions are responsible for this effect, and as a result, the value of the $\langle 4f|r|5d \rangle$ radial integral sensitively affects the calculated polarizability change.

I. INTRODUCTION

Four-wave mixing (FWM) has become an important technique in optical spectroscopy. It can provide information about the thermal and nonlinear-optical properties of materials, radiationless relaxation phenomena, and migration of mobile species such as charge carriers and excitons. One class of materials that has been studied by FWM is inorganic crystals and glasses doped with rare-earth[1-4] and transition-metal ions.[5-11] Many of these materials are important for solid-state laser applications, and the FWM results have been useful in understanding some aspects of their optical spectral dynamics. Prior work has generally involved relative measurements of FWM signal strengths and decay times, and have typically included only a limited scope of materials. The theoretical approach used to interpret much of the data has been based on the standard model developed for saturable two-level atomic systems.[12,13]

In order to enhance the understanding of the FWM signal observed for ions in solids, we have measured the absolute values of the signal strengths for an extensive series of oxide and fluoride glasses and crystals doped with Nd^{3+} ions. Comparing the observed FWM characteristics with theory indicates that the signal is associated with the difference in first-order susceptibilities of the Nd^{3+} ions in the excited state versus the ground state. A multilevel theoretical model is developed to interpret the results, and it is deduced that the $4f \rightarrow 5d$ transitions make the dominant contribution to the difference in the polarizabilities of the excited and ground states. The experimental results are therefore interpreted in terms of the magnitude of the $4f$-$5d$ radial integral, $\langle 4f|r|5d \rangle$, and the energy of the $4f \rightarrow 5d$ transition. This effect may have technological consequences of importance to laser materials since our previous work showed that, under certain pumping conditions, the induced polarizability change can alter the refractive index sufficiently, such that the "population lens" can become significant.[14]

II. THEORETICAL MODEL

The results of FWM experiments on crystals and glasses doped with rare-earth or transition-metal ions have previously been interpreted in terms of a model developed for other types of materials such as atomic vapors or photorefractive crystals. These models are based on saturable two-level atomic systems and, in general, they do not account for the properties of an optically pumped, multilevel system. We outline in this section the development of a model directly applicable to studies of four-wave mixing involving ions in solids.

One convenient formalism that describes FWM assumes that the scattering occurs from a laser-induced grating.[15,16] When two coherent laser beams are crossed inside a sample, a sinusoidal interference pattern results. The light interacts with the material to alter its optical constants with the same spatial period, and in this way produces a modulation of the susceptibility in the material,

$$\Delta\chi=\Delta\chi_0\sin[(\Delta\mathbf{k}\cdot\mathbf{z})] ,$$

where Δk is the difference of the wave vectors of the two beams. This modulation acts as a grating, and a beam entering the sample will undergo Bragg scattering off this grating. The intensity of this scattered signal beam I_s can be expressed as[15,16]

$$I_s=(\pi dT/2n\lambda)^2|\Delta\chi_0|^2 I_f\exp(-ad) , \quad (1)$$

where I_f is the intensity of the input beam, d is the sample thickness, a is the absorption coefficient, $\Delta\chi_0$ is the amplitude of the laser-induced change in the susceptibility at the wavelength λ, and T is the correction for sample surface reflectivity.

The interaction of the laser beams with the system of ions can be described in terms of the susceptibility with

$$\chi=\chi_g^{(1)}+(\chi_m^{(1)}-\chi_g^{(1)})(N_m/N)+\chi_g^{(3)}E_1E_2^*\ldots , \quad (2)$$

where the E_i fields and the impurity ion concentration N appear in the equation, and m and g denote the metastable and ground states, respectively. $\chi_m^{(1)}$ and $\chi_g^{(1)}$ are the susceptibilities of the sample if the ions are all in the excited or ground states, respectively. The first and last terms describe the linear and third-order susceptibilities. The second term represents the contribution from the "population grating," which depends on the difference in the first-order susceptibilities of the ions in their ground and metastable states. Since this term is proportional to N_m, which is in turn proportional to the square of the optical electric field of the incident waves, it is therefore a third-order susceptibility contribution.

It has been observed experimentally that the four-wave-mixing signal for ions in solids is many orders of magnitude greater when the laser is tuned to a resonant transition of the dopant ion, and that the signal observed under these conditions has the properties associated with scattering of the probe beam from a population grating. Furthermore, a calculation of the contribution of the signal associated with $\chi_g^{(3)}$ shows that this signal is negligible.[17] Thus, for resonant excitation conditions the effective nonlinear susceptibility arises solely from the second term in Eq. (2). Therefore, for a pumping rate of W and metastable state decay rate of β_{mg}, the susceptibility modulation amplitude due to the population grating, is

$$\Delta\chi=\tfrac{1}{2}|\chi_m^{(1)}-\chi_g^{(1)}|W(W+\beta_{mg})^{-1} . \quad (3)$$

Here, it is assumed that the ions that are excited relax rapidly to the metastable state, which has a much longer lifetime than any of the intermediate states of the relaxation process. Under these conditions, the change in susceptibility is a function only of the population in the metastable state.

The expression for $\Delta\chi$ can be derived by considering the transitions and energy levels shown in Fig. 1. For simplicity we make the assumption that the sample is being continuously pumped and the distribution of the population among the energy levels has reached equilibrium. It is assumed that all laser beams have the same frequency and phase-matching conditions are satisfied. The

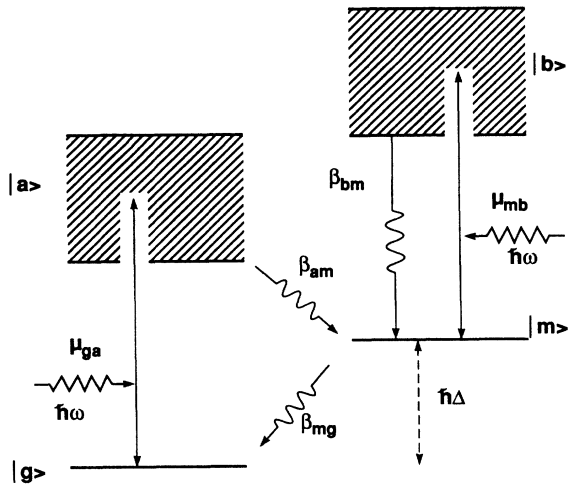

FIG. 1. Schematic energy level diagram for four-wave mixing of ions in crystals. $|g\rangle$ and $|m\rangle$ represent the ground and metastable states of the system, and $|a\rangle$ and $|b\rangle$ are higher-lying excited states. The dipole moments μ are indicated, as well as the relaxation rates β.

Nd^{3+} ion is a multilevel system, and the laser beams can interact with all possible transitions between these levels. Such a situation is too complex to treat exactly and has previously been regarded as a two-level system. The model developed here extends this treatment to four levels. The laser beams of frequency ω are allowed to interact with the ions in either the ground state $|g\rangle$ or the metastable state $|m\rangle$, which are separated in energy by an amount $\hbar\Delta$. The effects of all the excited states are incorporated into transitions to two effective excited states $|a\rangle$ and $|b\rangle$. The dipole moment operators μ_{ij} are shown in Fig. 1 along with the β_{ij} representing the decay rates for the excited levels.

The components of the density matrix for this system are determined by solving the Liouville-Schrödinger equation[18]

$$i\hbar\dot{\rho}=[H,\rho]+i\hbar(d\rho/dt)_{\text{decay}} . \quad (4)$$

The Hamiltonian for the system is given by

$$H=H_0+H_{\text{int}} , \quad (5a)$$

where

$$H_0=\begin{bmatrix}\varepsilon_g & 0 & 0 & 0\\ 0 & \varepsilon_a & 0 & 0\\ 0 & 0 & \varepsilon_m & 0\\ 0 & 0 & 0 & \varepsilon_b\end{bmatrix} \quad (5b)$$

and

$$H_{\text{int}}=\begin{bmatrix}0 & V_{ga} & 0 & 0\\ V_{ag} & 0 & 0 & 0\\ 0 & 0 & 0 & V_{mb}\\ 0 & 0 & V_{bm} & 0\end{bmatrix} . \quad (5c)$$

The interaction operator is given by $V_{ij}=-\mu_{ij}E_0$ with the electric field expressed as

$$E=E_0[\exp(-i\omega t)+\exp(i\omega t)]/2 ,$$

and the energies of the states are given by the ε_i. The susceptibility is calculated with

$$\chi=(4\pi N/E)\mathrm{Tr}(\underline{\mu}\,\underline{\rho}) , \tag{6a}$$

where

$$\mathrm{Tr}(\underline{\mu}\,\underline{\rho})=\rho_{ga}\mu_{ag}+\rho_{mb}\mu_{bm}+\rho_{ag}\mu_{ga}+\rho_{bm}\mu_{mb} . \tag{6b}$$

By assuming that $\beta_{am},\beta_{bm}\gg\beta_{mg}\gg W$, Eqs. (4) and (5) can be solved to give the relevant matrix elements:

$$\rho_{mm}=-\rho_{gg}\frac{|\mu_{ga}|^2T_{2,a}^{-1}E^2}{\hbar^2\beta_{mg}[(\omega_{ga}-\omega)^2+T_{2,a}^{-2}]} , \tag{7a}$$

$$\rho_{gg}=1-\rho_{mm} , \tag{7b}$$

$$\rho_{ga}=\rho_{gg}\frac{\mu_{ga}E}{\hbar[(\omega_{ga}-\omega)+iT_{2,a}^{-1}]} , \tag{7c}$$

$$\rho_{mb}=-\rho_{gg}\frac{\mu_{mb}E}{\hbar[(\omega_{mb}-\omega)+iT_{2,b}^{-1}]}\times\frac{|\mu_{ga}|^2T_{2,a}^{-1}E^2}{\hbar^2\beta_{mg}[(\omega_{ga}-\omega)^2+T_{2,a}^{-2}]} , \tag{7d}$$

where the T_2 terms are the dephasing times

$$T_{2,i}^{-1}=\beta_{ij}/2+\beta_{\mathrm{dephase}} . \tag{8}$$

We can recast Eqs. (7a)–(7d) to be in a form more similar to that of Eq. (3) by recognizing the presence of the pumping rate W in the equations

$$\rho_{mm}=W/\beta_{mg} , \tag{9a}$$

$$\rho_{gg}=1-\rho_{mm}\approx 1 , \tag{9b}$$

$$\rho_{ga}=\frac{\mu_{ga}E}{\hbar[(\omega_{ga}-\omega)+iT_{2,a}^{-1}]} , \tag{9c}$$

$$\rho_{mb}=(W/\beta_{mg})\frac{\mu_{mb}E}{\hbar[(\omega_{mb}-\omega)+iT_{2,b}^{-1}]} . \tag{9d}$$

Substituting Eqs. (9c) and (9d) into Eqs. (6) gives the expression for the magnitude of χ in the peak and valley regions, which can be used to calculate $\Delta\chi$ [see Eq. (3)]. Therefore, this result must be divided by two to give

$$\Delta\chi=\left[\frac{2\pi N_gW}{\beta_{mg}}\right]\left[\left[\frac{|\mu_{mb}|^2}{\hbar}\right]\left[\frac{(\omega_{mb}-\omega)-iT_{2,b}^{-1}}{(\omega_{mb}-\omega)^2+T_{2,b}^{-2}}+\frac{(\omega_{mb}+\omega)-iT_{2,b}^{-1}}{(\omega_{mb}+\omega)^2+T_{2,b}^{-2}}\right]-\left[\frac{|\mu_{ga}|^2}{\hbar}\right]\left[\frac{(\omega_{ga}-\omega)-iT_{2,a}^{-1}}{(\omega_{ga}-\omega)^2+T_{2,a}^{-2}}+\frac{(\omega_{ga}+\omega)-iT_{2,a}^{-1}}{(\omega_{ga}+\omega)^2+T_{2,a}^{-2}}\right]\right] . \tag{10}$$

The modulation of the real part of the susceptibility with respect to the average value well below saturation ($W\ll\beta_{mg}$), and far from resonance ($\omega_{ga}-\omega\gg T_{2,a}^{-1}$, $\omega_{mb}-\omega\gg T_{2,b}^{-1}$) is

$$\Delta\chi_R=(2\pi W\tau_mN_g/\hbar)\left[\frac{2\omega_{mb}|\mu_{mb}|^2}{\omega_{mb}^2-\omega^2}-\frac{2\omega_{ga}|\mu_{ga}|^2}{\omega_{ga}^2-\omega^2}\right] . \tag{11a}$$

Similarly, the imaginary part of Eq. (10) is

$$\Delta\chi_I=(2\pi W\tau_mN_g/\hbar)\left[\frac{|\mu_{mb}|^2T_{2,b}^{-1}}{(\omega_{mb}-\omega)^2+T_{2,b}^{-2}}-\frac{|\mu_{ga}|^2T_{2,a}^{-1}}{(\omega_{ga}-\omega)^2+T_{2,a}^{-2}}\right] . \tag{11b}$$

We have substituted the metastable emission lifetime $\tau_m=\beta_{mg}^{-1}$. In order to recast Eqs. (11a) and (11b) in terms of common physical parameters, it is useful to express the real and imaginary parts of the susceptibility, $\Delta\chi_R$ and $\Delta\chi_I$, in terms of the polarizability and the absorption cross section, α_p and σ, respectively. The polarizability arising from states i and j is defined by

$$\alpha_p(ij)=(2\omega_{ij}/\hbar)|\mu_{ij}|^2/(\omega_{ij}^2-\omega^2) , \tag{12a}$$

and the absorption cross section is given by

$$\sigma(ij)=(8\pi^2/n\hbar\lambda)\left[\frac{|\mu_{ij}|^2T_{2,j}^{-1}}{(\omega_{ij}-\omega)^2+T_{2,j}^{-2}}\right] . \tag{12b}$$

By substituting Eqs. (12) into (11), and by including the Lorentz local-field factor in the definition of the polarizability [$\mu_{ij}\rightarrow f_L\mu_{ij}$ where $f_L=(n^2+2)/3$], we obtain

$$\Delta\chi_R=2\pi f_L^2N_m\Delta\alpha_p \tag{13a}$$

and

$$\Delta\chi_I=n\lambda N_m\Delta\sigma/4\pi , \tag{13b}$$

where $\Delta\alpha_p=\alpha(m,b)-\alpha(g,a)$ and $\Delta\sigma=\sigma(m,b)-\sigma(g,a)$, and we note that $N_m=N_gW\tau_m$ for steady-state pumping if $W\ll\tau_m^{-1}$. The difference in the excited-state population that results from the interference of backward (b) and probe (p) beams, can be expressed in terms of

their intensities I_b and I_f to give

$$N_m = \frac{4(I_b I_p)^{1/2}\tau_m T}{h\nu d}[1-\exp(-ad)] , \quad (14)$$

where d is the sample thickness, a is the absorption coefficient, and T is the correction for sample reflectivity. By substituting Eqs. (14) and (13) into (1), we obtain the result

$$I_s = \frac{4\pi^2 T^2 f_L^2 \tau_m^2}{nhc} I_f I_b I_p \Delta\alpha_p^2 \exp(-ad)[1-\exp(-ad)]^2 \quad (15a)$$

for the phase grating, and

$$I_s = \left[\frac{\tau_m T^2}{2h\nu}\right]^2 I_f I_b I_p \Delta\sigma^2 \exp(-ad)[1-\exp(-ad)]^2 \quad (15b)$$

for the absorptive grating. Finally, by integrating over the transverse profiles of the input beams, and assuming that all of the beams are Gaussian with a radius of w_0 [i.e., $I = I_0 \exp(-2r^2/w_0^2)$] we obtain

$$P_s = \left[\frac{4}{3\pi^2 w_0^4}\right]\left[\frac{4\pi^2 T^2 f_L^2 \tau_m}{nhc}\right]^2 P_f P_b P_p \Delta\alpha_p^2 \exp(-ad) \times[1-\exp(-ad)]^2 \quad (16a)$$

and

$$P_s = \left[\frac{4}{3\pi^2 w_0^4}\right]\left[\frac{\tau_m T^2}{2h\nu}\right]^2 P_f P_b P_p \Delta\sigma^2 \exp(-ad) \times[1-\exp(-ad)]^2 \quad (16b)$$

for the phase and absorptive gratings, respectively, and P is the power. Taking the ratio of Eq. (16a) to (16b) and using typical values for $\Delta\sigma$ and an average value for $\Delta\alpha_p$ as discussed in the following it is found that the contribution to the signal from the absorptive grating, Eq. (16b), is much smaller than the contribution associated with the phase grating, Eq. (16a). Thus the contribution due to $\Delta\sigma$ is neglected. Similar calculations show that the signals due to thermal grating are negligible.[14,19,20] It should be noted that Eqs. (16) have been derived with the assumption that the small-spaced grating predominates over the large-spaced grating, since we have experimentally observed this to be the case This phenomenon may be due to the fact that only four fringes occur within the beam waist for the large-spaced grating, thereby reducing the intensity of the Bragg reflection compared to other higher-order diffraction spots. Lastly, we remark that Eqs. (16) agree with a previous calculation based on the theory of thick holograms.[14,16,21]

III. EXPERIMENT RESULTS

The samples used in this work involved a variety of oxide and fluoride glasses and crystals. Their compositions are listed in Table I. The relevant material properties, and our experimental results, are shown in Table II. Each sample was close to 3 mm in length, which is smaller than the overlap length of the laser beams. They had flat, parallel end faces with high-quality optical polishes.

An argon laser tuned to the 514.5-nm line served as the excitation source. For degenerate FWM, the laser output is split into three beams. Two of these were used as pump beams, which had equal intensities and traversed the sample in counter-propagating directions. The third beam was used as a probe beam. It had 20% the intensity of a pump beam, and entered the sample at an angle of about 2° to the forward pump beam. All the beams were chopped to reduce thermal loading of the sample. The signal was detected by a Si diode, sent through a preamplifier to a boxcar integrator, and output to an x-y recorder. The absolute laser beam power was measured with a calibrated thermopile, and the incident beam profile was determined by the knife-edge technique. The absolute phase-conjugate reflectivity was measured by replacing the sample with a mirror to reflect the probe beam back onto itself. The signal power was found to vary as the cube of the laser output power for several samples. This is consistent with the theoretical prediction of Eq. (16), and indicates that the results of the experiments are not affected by saturation or spurious contributions to the signals.

The theoretical expression for the FWM signal intensity due to the phase grating given by Eq. (16b) was used to obtain a value for the laser-induced change in polarizability for one particular sample, which is regarded as the "standard" sample. Our choice for the standard was the

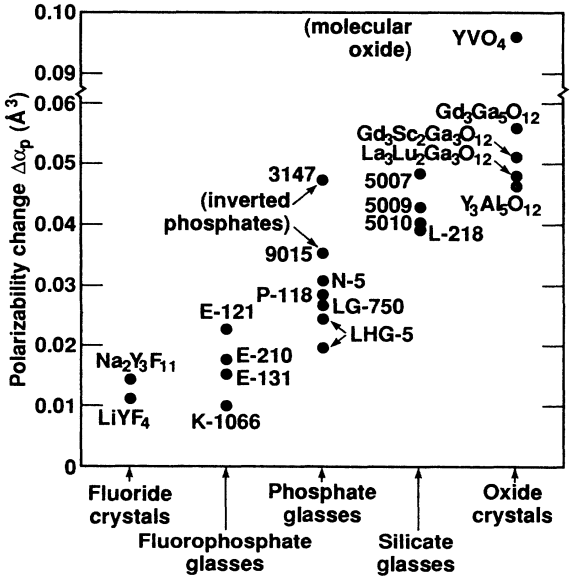

FIG. 2. Measurements of the polarizability change $\Delta\alpha_p$ of Nd^{3+} for the host materials studied in this work (see Tables I and II). The $\Delta\alpha_p$ values are clustered for each type of host. The fluorides give the smallest values, while the oxides give the largest.

phosphate glass sample No. 9015, since it had good optical quality and gave a strong signal. Using the values of τ_m, optical density, and n from Table II, and the measured values of $w_0=62$ μm, $P_f=P_b=0.31$ W, and $P_s/P_p=1.5\times10^{-4}$, we find that $\Delta\alpha_p=0.0354$ Å^3 for sample No. 9015. This quantity is estimated to be accurate to $\pm50\%$. In order to determine the $\Delta\alpha_p$ values for the rest of the samples, first the FWM signal magnitudes were determined relative to sample No. 9015, by alternating the unknown and the standard several times in the apparatus. Then the required corrections were applied for the given values of n, ad, and τ_m that characterized each sample. The results of this procedure are listed in the last column of Table II and are displayed in Fig. 2; the relative error among the samples is estimated to be $\pm20\%$. We mention that the emission lifetimes and optical densities appearing in Table II were directly measured for each sample used in this study. Average values of τ_m were derived for samples characterized by nonexponential decay; the absorption data were obtained with a Cary 17 spectrophotometer.

The main observation that is apparent from Table II and Fig. 2 is that the $\Delta\alpha_p$ values vary considerably for the different materials, although they have tended to cluster for each type of host material, be it fluoride, phosphate, silicate, or oxide. We see that the fluoride crystals and fluorophosphate glasses have the smallest values of $\Delta\alpha_p$ in the range of 0.01–0.02 Å^3, while the phosphate glasses give larger values of 0.02–0.03 Å^3. It is therefore not surprising that the fluorophosphate glass with the largest $\Delta\alpha_p$, E-121, is composed of an equal mixture of phosphate and fluoride constituents. Similarly, the phosphate glass with the greatest $\Delta\alpha_p$, sample No. 9015, is nearly 80% MgO. This glass is "inverted" since the modifier concentration is greater than that of the network former. The sample No. 9015 phosphate may behave as a material intermediate between an oxide and a phosphate, and therefore its $\Delta\alpha_p$ value will also be intermediate, as is

TABLE I. Nominal compositions of the glasses and crystals used in this work.

Designation	Composition (mol %)
Fluoride crystals:	
$Na_2Y_3F_{11}$	$Na_2Y_3F_{11}$
YLF	$LiYF_4$
Fluorophosphate glasses:	
K-1066	30.5 AlF_3, 7.6 MgF_2, 22.9 CaF_2, 7.6 SrF_2, 3.8 BaF_2, 3.8 $Ba(PO_3)_2$, 21.7 PbF_2, 2.0 NdF_3—NBS
E-131	2.7 $Al(PO_3)_3$, 37.3 AlF_3, 1 YF_3, 10 MgF_2, 30 CaF_2, 10 SrF_2, 8 BaF_2, 1 NdF_3—Owens-Illinois
E-210	2 $Al(PO_3)$, 38 AlF_3, 10 MgF_2, 30 CaF_2, 10 SrF_2, 10 BaF_2, 1 NdF_3—Owens-Illinois
E-121	47.9 $AlPO_4$, 51.4 NaF, 0.7 NdF3—Owens-Illinois
Phosphate glasses:	
LHG-5	Noya laser glass, 3 and 6 wt. % Nd_2O_3
LG-750	Schott laser glass
P-118	45 P_2O_5, 40 Li_2O, 10 CaO, ~4 Al_2O_3, ~1 Nd_2O_3—Kigre
N-5	41 P_2O_5, 29 Na_2O, 11 Li_2O, 11 Nb_2O_5, 8 Al_2O_3, Nd_2O_3—Kigre
Inverted phosphate glasses (mostly oxide):	
9015	21.9 P_2O_5, 77 MgO, 0.3 As_2O_3, 0.8 Nd_2O_3—Westinghouse
3147	21.8 P_2O_5, 77.5 TeO_2, 0.8 Nd_2O_3—Kigre
Silicate glasses:	
5009	65 SiO_2, 15 K_2O, 20 CaO, 0.3 Nd_2O_3—Hoya
5010	65 SiO_2, 15 K_2O, 20 SrO, 0.3 Nd_2O_3—Hoya
5007	65 SiO_2, 15 K_2O, 20 BaO, 0.3 Nd_2O_3—Hoya
L-218	39.1 SiO_2, 24.8 BaO, 35.4 TiO_2, 0.7 Nd_2O_3—NBS
Oxide crystals:	
YAG	$Y_3Al_5O_{12}$
GGG	$Gd_3Ga_5O_{12}$
GSGG	$Gd_3Sc_2Ga_3O_{12}$
LLGG	$La_3Lu_2Ga_3O_{12}$
YVO_4	YVO_4

observed here. The silicate glasses provide $\Delta\alpha_p$ values clustered near 0.04–0.05 Å^3, while the Nd-doped oxide garnets are found to give values of 0.045–0.055 Å^3. Lastly, the YVO_4 sample gave the largest result of $\Delta\alpha_p = 0.096$ Å^3. While we can gain confidence in our experimental method owing to the clustering of the $\Delta\alpha_p$ values of similar materials, the question remains as to what physical mechanisms actually influence the magnitude of $\Delta\alpha_p$. This question will be addressed in the next section.

IV. DISCUSSION

In the preceding section, the experimentally measured values of the change in the polarizability of the $^4F_{3/2}$ excited state of Nd^{3+}, compared to that of the $^4I_{9/2}$ ground state ($\Delta\alpha_p$) were provided for a wide variety of host materials. By referring back to Fig. 2, it is clear that there are two main experimental observations that need to be theoretically evaluated: (1) the absolute magnitude of the $\Delta\alpha_p$ values, and (2) the basis for the variation among the different host material classes.

In order to interpret the data, we return to the original ideas proposed by Judd to explain the intensities of the $4f \rightarrow 4f$ transitions.[22] Here it was recognized that the $4f \rightarrow 4f$ transitions would "borrow" intensity from the $4f \rightarrow 5d$ and $4f \rightarrow ng$ transitions. Therefore, the nonresonant $4f^2 5d$ and $4f^2 ng$ states are collectively recognized as the $|a\rangle$ and $|b\rangle$ states of Eq. (11a). The relevant energy levels are depicted in Fig. 3, where the $^4F_{3/2}$ and $^4I_{9/2}$ $4f^3$ states are shown relative to the approximate positions of the $4f^2 5d$ and $4f^2 ng$ manifolds (assumed to be at the ionization limit). Using Eq. (12a), the polarizability change can be expressed as

TABLE II. Polarizability changes and relevant optical properties of samples used in this work.

Sample designation	Refractive index n	Optical density at 514 nm	Emission lifetime τ_m (μs)	Polarizability change $\Delta\alpha_p$ (Å^3)
Fluoride crystals:				
$Na_2Y_3F_{11}$	1.45	0.108	316	0.0107
$LiYF_4$	1.46	0.075	371	0.0143
Fluorophosphate glasses:				
K-1066	1.53	0.215	180	0.0101
E-131	1.44	0.090	430	0.0151
E-210	1.43	0.088	401	0.0175
E-121	1.49	0.093	369	0.0228
Phosphate glasses:				
LHG-5	1.54	0.263	267	0.0195
	1.54	0.143	338	0.0239
LG-750	1.55	0.115	341	0.0265
P-118	1.55	0.260	175	0.0283
N-5	1.58	0.153	193	0.0307
Inverted phosphate glasses:				
9015	1.52	0.116	230	0.0354 (calibration)
3147	2.06	0.047	245	0.0474
Silicate glasses:				
5009	1.54	0.044	446	0.0430
5010	1.55	0.039	462	0.0406
5007	1.57	0.038	452	0.0484
L-218	1.72	0.130	167	0.0396
Oxide crystals:				
$Y_3Al_5O_{12}$	1.82	0.060	214	0.0464
$Gd_3Ga_5O_{12}$	1.97	0.030	236	0.0563
$Gd_3Sc_2Ga_3O_{12}$	1.97	0.128	132	0.0513
$La_3Lu_2Ga_3O_{12}$	1.96	0.092	182	0.0483
YVO_4[a]	1.87	0.149	60	0.096

[a]Average of two polarizations.

$$\Delta\alpha_p^{(nl)}=\frac{\tilde{\nu}_0^{(nl)}\alpha_{FS}}{\pi}\left[\frac{|\langle 4f^3,{}^4F_{3/2}|Z|4f^2nl\rangle|^2}{(\tilde{\nu}_0^{(nl)}-\tilde{\nu}_{ex})^2-\tilde{\nu}^2}-\frac{|\langle 4f^3,{}^4I_{9/2}|Z|4f^2nl\rangle|^2}{(\tilde{\nu}_0^{(nl)})^2-\tilde{\nu}^2}\right], \tag{17}$$

where $\tilde{\nu}_0^{(nl)}$ is the average energy of the $4f^2nl$ states ($nl=5d$ or ng) in cm^{-1}, $\tilde{\nu}_{ex}$ is the energy of the ${}^4F_{3/2}$ state, $\tilde{\nu}$ is the energy of the laser photon, $Z=\sum_{i=1}^{3}z_i$ is the position coordinate for the $i=3$ $4f$ electrons, and α_{FS} is the fine-structure (FS) constant. The sum over all states of the $4f^2nl$ configuration is implied. According to Axe, the sum of the transition moments over the entire $nl=5d$, ng manifold is independent of the identity if the $4f^3$ state (i.e., ${}^4F_{3/2}$ or ${}^4I_{9/2}$), and can be written as[23]

$$|\langle 4f^3,LSJM|Z|4f^2nl\rangle|^2=\frac{l+4}{6\sqrt{7}}|\langle 4f|r|nl\rangle|^2\langle 4f^3LSJM|U_0^{(0)}|4f^3LSJM\rangle, \tag{18}$$

where the unit tensor is given by

$$\langle 4f^3LSJM|U_0^{(0)}|4f^3LSJM\rangle=\frac{3}{\sqrt{7}}. \tag{19}$$

(We note that the terms containing the $U_0^{(2)}$ tensors interfere to zero upon summing over the magnetic sublevels of the JM state.) Substituting Eqs. (19) and (18) into (17) yields

$$\Delta\alpha_p^{(5d)}=\frac{3\tilde{\nu}_0^{(5d)}\alpha_{FS}}{7\pi}|\langle 4f|r|5d\rangle|^2\left[\frac{1}{(\tilde{\nu}_0^{(5d)}-\tilde{\nu}_{ex})^2-\tilde{\nu}^2}-\frac{1}{(\tilde{\nu}_0^{(5d)})^2-\tilde{\nu}^2}\right] \tag{20}$$

for the $4f^25d$ states, while the result for the $4f^2ng$ states is

$$\Delta\alpha_p^{(ng)}=\frac{4\tilde{\nu}_0^{(ng)}\alpha_{FS}}{7\pi}|\langle 4f|r|ng\rangle|^2\left[\frac{1}{(\tilde{\nu}_0^{(ng)}-\tilde{\nu}_{ex})^2-\tilde{\nu}^2}-\frac{1}{(\tilde{\nu}_0^{(ng)})^2-\tilde{\nu}^2}\right]. \tag{21}$$

The question arises as to what values to insert into Eqs. (20) and (21). The first inclination is to utilize free-ion values since they are available.[22] The lowest $4f^25d$ level of free-ion Nd^{3+} is known to be at 71 500 cm^{-1},[24] and therefore the median energy of the $4f^25d$ manifold is at about 80 000 cm^{-1}, owing to the 20 000 cm^{-1} splitting of the $4f^2$ core. The $\langle 4f|r|5d\rangle$ radial integral has been calculated by Rajnak and co-workers and found to be 0.39 Å.[25] Using $\tilde{\nu}_{ex}=11\,500$ cm^{-1} and $\alpha_{FS}=137^{-1}$, we calculate that $\Delta\alpha_p^{(5d)}=0.080$ Å.[3] This magnitude is near the largest $\Delta\alpha_p$ values that were measured.

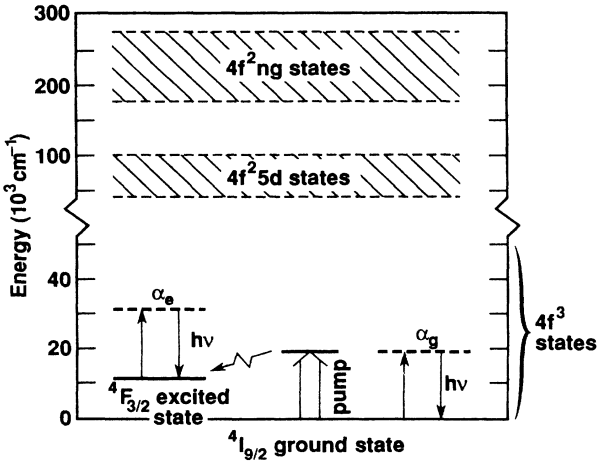

FIG. 3. Energy level diagram appropriate to the Nd^{3+} impurity. The relevant $4f^3$ states are shown, as well as the higher-lying $4f^25d$ and $4f^2ng$ states from which the polarizability change arises.

Following Judd,[22] it is assumed that the $4f^2ng$ states appear near the ionization limit of 267 000 cm^{-1}, and the $\langle 4f|r|ng\rangle$ integral is approximated as $\langle 4f|r^2|4f\rangle^{1/2}=0.55$ Å (assuming closure). This gives $\Delta\alpha_p^{(ng)}=0.014$ Å^3, a magnitude considerably smaller than $\Delta\alpha_p^{(5d)}=0.080$ Å^3. Since these free-ion calculations suggest that the $5d$ contribution is much larger than that of the ng, the ensuing discussion focuses on the nature of the $4f\rightarrow 5d$ interactions.

The calculated result obtained on the basis of the free-ion wave functions is that $\Delta\alpha_p^{(5d)}=0.080$ Å^3. Experimentally, mean values of 0.014, 0.026, 0.043, and 0.051 Å^3 have been measured for the fluorides, phosphates, silicates, and oxides, respectively. The important observations are that all of the materials give $\Delta\alpha_p$ values smaller than that of the theoretical calculation, and that there is a strong host dependence. The two variables of Eq. (20) that contain the information about the electronic structure of Nd^{3+} are the radial integral $\langle 4f|r|5d\rangle$ and the average energy of the $4f^25d$ states, $\tilde{\nu}_0^{(5d)}$. The main question that arises is whether the experimental variability of $\Delta\alpha_p$ can be predominantly accounted for in terms of the variation of the $\nu_0^{(5d)}$ or the $\langle 4f|r|5d\rangle$ parameter. Insight into this question can be gained by examining Fig. 4, where the average $\Delta\alpha_p$ value for each type of host material has been reported as one of a family of curves, on a plot of $\langle 4f|r|5d\rangle$ versus $\tilde{\nu}_0^{(5d)}$. In this way, we can determine which parameter can most reasonably account for

the differences between the free-ion value (shown as a point in Fig. 4), and those of the different hosts. From Fig. 4, we can see that moving vertically from the free-ion point requires that the energy denominator be increased from $\bar{\nu}_0^{(5d)}=80\,000$ to 96 000 cm^{-1} for the oxide hosts, and to $>>120\,000$ cm^{-1} for the fluorides. It is known that this extent of variation in $\bar{\nu}_0$ is unreasonable, on the basis of the known absorption spectra of the rare-earth ions. In particular, it is known that for the Ce^{3+} impurity the average position of the $4f\rightarrow 5d$ bands is near, and sometimes even less than, the free-ion position.[26,27]

The other possibility that is apparent from Fig. 4 is that the radial integral may be reduced for the Nd^{3+} ions incorporated into a host, compared to the free ion (represented by a horizontal excursion from the free-ion point in Fig. 4). There is considerable evidence which suggests that this may be a reasonable idea. For example, it has been noted that the observed $4f\rightarrow 5d$ transition strengths tend to be significantly less than anticipated on the basis of the free-ion wave functions.[28,29] Similarly, electronic Raman data have been interpreted to indicate that the magnitudes of the $5d$ and ng contributions were comparable.[30]

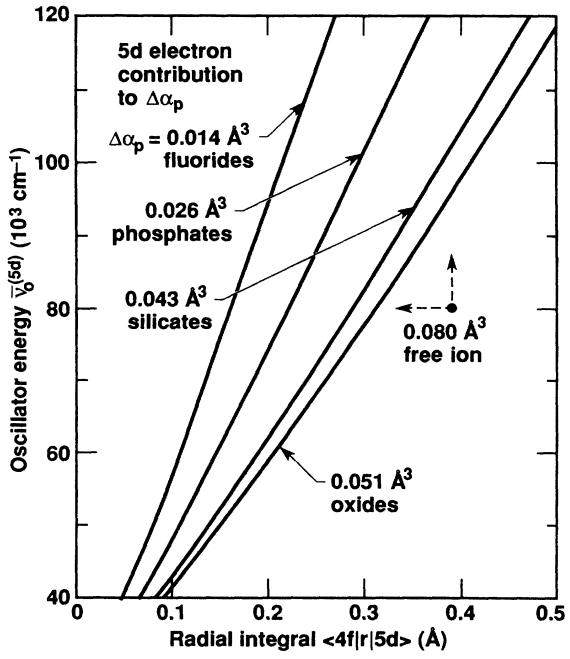

FIG. 4. Family of curves representing the corresponding values of the radial integral $\langle 4f|r|5d\rangle$ and the $4f^2 5d$ energy $\bar{\nu}_0^{(5d)}$ that, when substituted into Eq. (20), yield the mean measured values of $\Delta\alpha_p$ for the fluoride, phosphate, silicate, and oxide hosts. The point representing free-ion value is also shown. It is suggested that the variation of $\bar{\nu}_0^{(5d)}$ cannot account for the differences in the $\Delta\alpha_p$ for the free ion and the various host materials (vertical dashed arrow), while the variation of the $\langle 4f|r|5d\rangle$ integral provides the most reasonable explanation (horizontal dashed arrow).

Krupke was the first to quantitatively demonstrate that the $5d$ contributions to the $4f\rightarrow 4f$ oscillator strengths were considerably smaller than predicted from the free-ion wave functions.[31] In this work, the absorption spectra of numerous rare earths in Y_2O_3 were obtained, and analyzed using Judd-Ofelt theory.[22,32] The odd-parity components of the crystal-field potential were calculated, and with this information it was shown that the derived value of the $\langle 4f|r|5d\rangle$ radial integral was markedly smaller than that of the free ion. It was noted by Krupke that the $4f$ orbital does not have any nodes, while the $5d$ orbital must exhibit two. Examination of the $4f$ and $5d$ wave functions of Rajnak reveals that the $5d$ node occurs near the peak of the probability distribution for the $4f$ wave function,[33] and we may therefore suspect that the $\langle 4f|r|5d\rangle$ radial integral will be sensitive to perturbations of these wave functions. The $5d$ wave function may be substantially altered by the electrostatic field and the bonding of the host. This effect may account for the strong host dependence that we have observed.

The host dependence observed here is corroborated by recent two-photon absorption results.[34] In these experiments, the absolute values of the two-photon cross sections were measured for Nd^{3+} in $Y_3Al_5O_{12}$ and $LiYF_4$, and then related to the $\langle 4f|r|5d\rangle$ radial integral. Using the free-ion value of $\nu_0^{(5d)}=80\,000$ cm^{-1}, the two-photon experiments provide the derived magnitudes of the $\langle 4f|r|5d\rangle$ parameter as 0.47 Å and 0.26 Å for Nd^{3+} in $Y_3Al_5O_{12}$ and $LiYF_4$, respectively, to be compared to the respective values of 0.30 Å and 0.17 Å obtained from the present FWM experiments [see Table II and Eq. (20)]. We find the agreement to be satisfactory, in consideration of the absolute accuracy of the two experiments. Moreover, the ratio of the radial integrals for the $Y_3Al_5O_{12}$ and $LiYF_4$ hosts is found to be in excellent agreement, indicating that the host dependence that we have observed is corroborated well by both experimental techniques.

In the preceding discussion, the variations of $\Delta\alpha_p$ have been interpreted in terms of changes of the $\langle 4f|r|5d\rangle$ radial integral. There are, however, other reasonable interpretations that should be considered.[30] For example, the $4f\rightarrow 5d$ transition may be strongly mixed with charge-transfer transitions (in which an electron is transferred from the host anion to the impurity ion). This explanation has the additional merit that it can provide a rationale as to why the oxides have the largest $\Delta\alpha_p$ values, since the charge-transfer transitions are expected to be stronger and at lower energies in oxides, compared to other materials. This same type of situation was found to exist for Cr^{3+}-doped crystals.[21] A similar type of mechanism has been discussed by Reid and Richardson to account for the two-photon absorption strength of rare-earth ion impurities.[35] They have proposed that a virtual transition occurs on the ligand, and for this reason, find that the polarizability of the ligand plays an important role in determining the strength of the two-photon transition. In addition, another possibility is that the role of the g electrons may be more important than originally suspected, since they are likely to be strongly mixed with the wave functions of the neighboring anions. Other issues that need to be considered involve the structure and

relaxation of the host at the impurity site. For instance, the continuous random network skeletal structure of silicate glasses is generally more rigid than the linear chain structure of phosphate glasses.[36] The amount of relaxation, and the proximity and number of nearest neighbors to the Nd^{3+} ion, may impact the magnitude of the radial integral.

The one very different sample investigated in this work is YVO_4:Nd^{3+}, which was found to have a large value of $\Delta\alpha_p$ as shown in Fig. 2. This crystal can be thought of as being made up of VO_4^{3-} tetrahedra. The Nd^{3+} ions will enter the lattice substitutionally for the Y^{3+} ions, and their polarizability will be affected by the neighboring vanadate molecular ion. The VO_4^{3-} ions exhibit strong molecular orbital transitions in the near ultraviolet spectra;[37] these low-lying transitions may render the vanadate species to be very polarizable.

V. CONCLUSIONS

In this work, we have derived a method by which to measure the difference in the polarizability $\Delta\alpha_p$ of the Nd^{3+} impurities in the $^4F_{3/2}$ metastable excited state, compared to the $^4I_{9/2}$ ground state. To do this, four-wave-mixing experiments have been conducted in a quantitative manner, so as to obtain absolute values of the polarizability change, $\Delta\alpha_p$; the density matrix formalism was used in conjunction with thick hologram theory to develop the appropriate equation needed to analyze the results. It was found that $\Delta\alpha_p$ exhibited a great deal of host dependence, with fluorides, phosphates, silicates, and oxides giving average values of 0.014, 0.026, 0.043, and 0.051 Å^3 for $\Delta\alpha_p$. On the basis of the free-ion wave functions and the assumption that the $4f^25d$ states provide the main intermediate states that give rise to the polarizability change, it is calculated that $\Delta\alpha_p^{(5d)}=0.080$ Å^3. We have interpreted the discrepancy between the free-ion and impurity values of $\Delta\alpha_p$, and the variation among the host materials, as being due to the sensitivity of the $\langle 4f|r|5d\rangle$ radial integral to the host environment. This sensitivity is caused by the interference effects that arise from the coincidence of the node of the $5d$ wave function with the peak of the $4f$ wave function probability distribution.

ACKNOWLEDGMENTS

This research was performed under the auspices of the Division of Materials Sciences of the Office of Basic Energy Sciences, U.S. Department of Energy, and the Lawrence Livermore National Laboratory under Contract No. W-7405-ENG-48. Additional support was provided for R. C. Powell by the National Science Foundation under Grant No. DMR-87-22350. We wish to thank Eberhard Prochnow for polishing all of the samples used in the experiments.

*Permanent address: Department of Physics, Oklahoma State University, Stillwater, OK 74078-0444.

[1]C. M. Lawson, R. C. Powell, and W. K. Zwicker, Phys. Rev. B **26**, 4836 (1982); J. K. Tyminski, R. C. Powell, and W. K. Zwicker, *ibid.* **29**, 6074 (1984); R. C. Powell, J. K. Tyminski, A. M. Ghazzawi, and C. M. Lawson, IEEE J. Quantum Electron. **QE-22**, 1355 (1986).

[2]G. P. Morgan, S. Chen, and W. M. Yen, IEEE J. Quantum Electron. **QE-22**, 1360 (1986).

[3]R. W. Boyd, M. T. Gruneisen, P. Narum, D. J. Simkin, B. Dunn, and D. L. Yang, Opt. Lett. **11**, 162 (1986).

[4]S. C. Rand, J. F. Lam, R. S. Turley, R. A. McFarlane, and O. M. Stafsudd, Phys. Rev. Lett. **59**, 597 (1987).

[5]H. Eichler, G. Salje, and H. Stahl, J. Appl. Phys. **44**, 5383 (1973); H. J. Eichler, J. Eichler, K. Knof, and Ch. Noack, Phys. Status Solidi A **52**, 481 (1979); H. Eichler, P. Glozbach, and B. Kluzowski, Z. Angew. Phys. **28**, 303 (1970).

[6]K. O. Hill, Appl. Opt. **10**, 1695 (1969).

[7]P. F. Liao and D. M. Bloom, Opt. Lett. **3**, 4 (1978); P. F. Liao, L. M. Humphrey, D. M. Bloom, and S. Geschwind, Phys. Rev. B **20**, 4145 (1979).

[8]D. S. Hamilton, D. Heiman, J. Feinberg, and R. W. Hellwarth, Opt. Lett. **4**, 124 (1979).

[9]D. G. Steel and S. C. Rand, Phys. Rev. Lett. **55**, 2285 (1985); D. G. Steel, S. C. Rand, and J. Liu, J. Opt. Soc. Am. B **4**, 1794 (1987).

[10]T. Catunda, J. P. Andreeta, and J. C. Castro, Appl. Opt. **25**, 2391 (1986); T. Catunda and J. C. Castro, Opt. Commun. **63**, 185 (1987).

[11]A. Suchocki, J. D. Allen, R. C. Powell, and G. M. Loiacono, Phys. Rev. B **36**, 6729 (1987); A. M. Ghazzawi, J. K. Tyminski, R. C. Powell, and J. C. Walling, *ibid.* **30**, 7182 (1984); A. Suchocki, G. D. Gilliland, and R. C. Powell, *ibid.* **35**, 5830 (1987); G. D. Gilliland, A. Suchocki, K. W. Ver Steeg, R. C. Powell, and D. F. Heller, *ibid.* **38**, 6227 (1988); A. Suchocki and R. C. Powell, Chem. Phys. **128**, 59 (1988); G. J. Quarles, A. Suchocki, R. C. Powell, and S. Lai, Phys. Rev. B **38**, 9996 (1988); F. M. Durville, R. C. Powell, G. Boulon, and B. Champagnon, *ibid.* **37**, 1435 (1988).

[12]R. L. Abrams and R. C. Lind, Opt. Lett. **2**, 94 (1978).

[13]A. Yariv and D. M. Pepper, Opt. Lett. **1**, 16 (1977).

[14]R. C. Powell, S. A. Payne, L. L. Chase, and G. D. Wilke, Opt. Lett. **14**, 1204 (1989).

[15]H. J. Eichler, P. Gunter, and D. W. Pohl, *Laser-Induced Dynamic Gratings* (Springer-Verlag, Berlin, 1986).

[16]H. Kogelnik, Bell Syst. Tech. J. **48**, 2909 (1969).

[17]G. B. Al'tshuler and S. A. Koslov, Kvant. Elektron. (Moscow) **12**, 698 (1985) [Sov. J. Quantum Electron. **15**, 459 (1985)].

[18]Y. R. Shen, *The Principles of Nonlinear Optics* (Wiley, New York, 1984); M. D. Levenson, *Introduction to Nonlinear Laser Spectroscopy* (Academic, New York, 1982).

[19]G. Martin and R. W. Hellwarth, Appl. Phys. Lett. **34**, 371 (1979).

[20]H. Eichler, G. Enterlein, J. Munschau, and H. Stahl, Z. Angew. Phys. **31**, 1 (1970).

[21]S. C. Weaver and S. A. Payne, Phys. Rev. B **40**, 10 727 (1989).

[22]B. R. Judd, Phys. Rev. **127**, 750 (1962).

[23]J. D. Axe, Jr., Phys. Rev. **136**, A42 (1964).

[24]L. Brewer, J. Opt. Soc. Am. **61**, 1666 (1971).

[25]W. T. Carnall, J. V. Beitz, H. Crosswhite, K. Rajnak, and J. B. Mann, in *Systematics and the Properties of Lanthanides,* edited by S. P. Sinha (Kluwer, Hingham, 1983).

[26]S. P. Chernov, L. I. Devyatkova, O. N. Ivanova, A. A. Kaminskii, V. V. Mikhailin, S. N. Rudnev, and T. V. Uvaro-

va, Phys. Status Solidi A **88**, K169 (1985).
[27]B. F. Aull and H. P. Jenssen, Phys. Rev. B **34**, 6640 (1986); **34**, 6647 (1986).
[28]B. R. Judd, Inorg. Chim. Acta **139**, 341 (1987).
[29]G. M. Williams, N. Edelstein, L. A. Boatner, and M. M. Abraham, Phys. Rev. B **40**, 4143 (1989).
[30]P. C. Becker, N. Edelstein, B. R. Judd, R. C. Leavitt, and G. M. S. Lister, J. Phys. C **18**, L1063 (1985).
[31]W. F. Krupke, Phys. Rev. **145**, 325 (1966).
[32]G. S. Ofelt, J. Chem. Phys. **37**, 511 (1962).
[33]K. Rajnak, J. Chem. Phys. **37**, 2440 (1962).
[34]L. L. Chase and S. A. Payne, Phys. Rev. B **34**, 8883 (1986).
[35]M. F. Reid and F. S. Richardson, Phys. Rev. B **29**, 2830 (1984).
[36]N. E. Alekseev, V. P. Gapontsev, M. E. Zhabotinskii, V. B. Kravchenko, and Yu. P. Rudnitskii, *Laser Phosphate Glasses* (Nanka, Moscow, 1983).
[37]G. Blasse, Philips Res. Rep. **23**, 344 (1968); **24**, 131 (1969).